# A hybrid approach to invertebrate biomonitoring using computer vision and DNA metabarcoding

Jarrett D. Blair [1,2], Michael D. Weiser [3], Cameron Siler [3,4], Michael Kaspari [3,5], Sierra N. Smith [3,4,6], J. F. McLaughlin [3,4,7], Katie E. Marshall [1]

[1] Department of Zoology, University of British Columbia, Vancouver, BC V6T 1Z4, Canada
[2] Department of Ecoscience, Aarhus University, 8000 Aarhus C, Denmark
[3] School of Biological Sciences, University of Oklahoma, Norman, OK 73019-0235, USA
[4] Sam Noble Oklahoma Museum of Natural History, University of Oklahoma, Norman, OK 73072-7029, USA
[5] Conservation Ecology Center, Smithsonian's National Zoo and Conservation
[6] Department of Biology Institute, Front Royal, VA 22630, University of Texas at Arlington, Arlington, TX, 76019, USA.
[7] Department of Biological Sciences, University of Alaska Anchorage, Anchorage, AK, 99508, USA.

Corresponding author: Jarrett Blair, Department of Ecoscience, Aarhus University, C.F. Møllers Allé 8, 8000 Aarhus C, Denmark, jarrett@ecos.au.dk

**Abstract**

1. Automated invertebrate classification using computer vision has shown significant potential to improve specimen processing efficiency. However, challenges such as invertebrate diversity and morphological similarity among taxa can make it difficult to infer fine-scale taxonomic classifications using computer vision. As a result, many invertebrate computer vision models are forced to make classifications at coarser levels, such as at family or order.
2. Here we propose a novel framework to combine computer vision and bulk DNA metabarcoding specimen processing pipelines to improve the accuracy and taxonomic granularity of individual specimen classifications. To improve specimen classification accuracy, our framework uses multimodal fusion models that combine image data with DNA-based assemblage data. To refine the taxonomic granularity of the model's classifications, our framework cross-references the classifications with DNA metabarcoding detections from bulk samples. We demonstrated this framework using a continental-scale, invertebrate bycatch dataset collected by the National Ecological Observatory Network. The dataset included 17 taxa spanning three phyla (Annelida, Arthropoda, and Mollusca), with the finest starting taxonomic granularity of these taxa being order-level.
3. Using this framework, we reached a classification accuracy of 79.6% across the 17 taxa using real DNA assemblage data, and 83.6% when the assemblage data was "error-free", resulting in a 2.2% and 6.2% increase in accuracy when compared to a model trained using only images. After cross-referencing with the DNA metabarcoding detections, we

improved taxonomic granularity in up to 72.2% of classifications, with up to 5.7% reaching species-level.

4. By providing computer vision models with coincident DNA assemblage data, and refining individual classifications using DNA metabarcoding detections, our framework has the potential to greatly expand the capabilities of biological computer vision classifiers. This framework allows computer vision classifiers to infer taxonomically fine-grained classifications when it would otherwise be difficult or impossible due to challenges of morphologic similarity or data scarcity. This framework is not limited to terrestrial invertebrates and could be applied in any instance where image and DNA metabarcoding data are concurrently collected.

## 1. Introduction

Computer vision has the potential to transform invertebrate ecology by automating estimations of invertebrate abundance, biomass, and diversity (Høye *et al.*, 2021; Schneider *et al.*, 2022). However, accurately classifying invertebrate species using computer vision is challenging. This is partly due to the sheer diversity of invertebrates, as there are an estimated 7.5 million (~1.5 million named) terrestrial invertebrates species globally (Stork, 2018). This has led most invertebrate classification models to opt for coarser taxonomic granularity (e.g. order-level instead of species-level classifications) with relatively few unique classification groups (usually <50; (Ärje *et al.*, 2020; Blair *et al.*, 2022; Schneider *et al.*, 2022). However, ecology studies can involve hundreds or thousands of species, which poses a challenge for simpler machine vision techniques.

One way computer vision models have overcome the challenge of handling many thousands or millions of classification labels is by including additional data modalities such as contextual metadata (e.g. collection location) in computer vision models. The mobile app iNaturalist uses this spatiotemporal data in combination with user-submitted photos to classify nearly 80,000 taxa across the tree of life (Leary *et al.*, 2023). Other studies conducted on a smaller scale have also found substantial improvements to classification accuracy with multimodal models that include both metadata and images compared to image-only models (Berg *et al.*, 2014; Terry, Roy and August, 2020; Blair *et al.*, 2022). However, despite the potential improvements in accuracy, there are several pitfalls to consider when including spatiotemporal metadata in a computer vision model. For one, spatiotemporal metadata is a lagging indicator of species habitat occupancy (i.e. the presence or absence of a species at a given place and time), and as such it is susceptible to data drift over time (Friedland, 2024). That is, spatiotemporal distributions of taxa

change over time, but computer vision models can only learn from past data. Unless a computer vision model is updated frequently with more recent data, the species range distributions it has learned may quickly become outdated. Finally, when dealing with many machine learning classes, spatiotemporal metadata does not solve the challenge of gathering enough training data to sufficiently train a computer vision model (Beery, Van Horn and Perona, 2018; Beery *et al.*, 2020). In short, studies that incorporate spatiotemporal metadata have shown that supplemental, non-visual data can improve ecological computer vision models, but spatiotemporal metadata itself has several potential drawbacks. In this study, we leverage an alternative data stream that does not pose the same challenges associated with spatiotemporal metadata: DNA metabarcoding.

DNA metabarcoding is an established tool in ecological research that allows for multiple species to be identified from a single sample using high-throughput sequencing (Deiner et al., 2017; Liu et al., 2020; Taberlet et al., 2012). Using this method, DNA can be collected from the environment (eDNA) or from preservative media (e.g. ethanol in insect bycatch samples), sequenced, and then used to infer ecological metrics such as species richness and community composition (Wood *et al.*, 2017; Marquina *et al.*, 2019; Weiser *et al.*, 2022). Due to its improved cost-effectiveness, DNA metabarcoding is becoming more frequently used in large-scale studies where traditional morphological identification techniques cannot keep up financially or logistically (Liu et al., 2020). However, despite being an excellent tool for detecting occurrence at fine taxonomic granularity (even below species-level; Stewart & Taylor, 2020; Wilcox et al., 2015), DNA metabarcoding cannot be used to reliably estimate species abundance or biomass (Bista *et al.*, 2018; Lamb *et al.*, 2019). Instead, eDNA metabarcoding is more suitable for binary presence/absence detections of species. Additionally, while DNA metabarcoding is generally

reliable for taxonomic identifications, it is not exempt from false positive and false negative detections (Guillera-Arroita *et al.*, 2017). Some examples of how this may occur include DNA contamination and primer mis-priming (false-positives), or DNA degradation and insufficient sampling effort (false-negatives) (Guillera-Arroita *et al.*, 2017; Liu *et al.*, 2020). Therefore, while DNA metabarcoding offers considerable advantages for biodiversity assessment (e.g., species inventories, species richness) its limitations often necessitate the use of complementary indicators such as visual observations for other metrics (e.g., abundance, biomass) (Schneider et al., 2022).

Given DNA metabarcoding's ability to produce reliable fine-scale community composition data, and computer vision's ability to measure abundance and biomass at coarse taxonomic granularity, several studies have called for a synergistic classification pipeline that takes advantage of the strengths of each tool (Badirli et al., 2023; Schneider et al., 2022; Sys et al., 2022). In theory, such a pipeline could leverage DNA metabarcoding's fine taxonomic granularity against computer vision's ability to infer specimen-level characteristics (identity, morphology, etc.) to make ecological inferences that would not be possible using either data stream on their own. DNA might also be a favourable alternative to spatiotemporal metadata, as it is a more direct and coincident indicator of species habitat occupancy, likely making it more resistant to data drift over time (Taberlet *et al.*, 2018). Despite the potential benefits of multimodal image-DNA classification models for ecological research, few studies have explored this approach. Additionally, proposed hybrid classification pipelines either leave the DNA and image data streams separate (Sys *et al.*, 2022), or sequence specimens individually, and thus do not take advantage of metabarcoding's ability to process bulk samples (Badirli *et al.*, 2023).

Here we present a novel approach for identifying and classifying invertebrate taxa which integrates DNA metabarcoding and computer vision. The objective of this hybrid approach is to improve the accuracy and taxonomic granularity of computer vision classifications by adding concurrent community assemblage data derived from DNA metabarcoding into a bulk specimen classification pipeline (Figure 1). The combination of DNA and image data occurs twice throughout the pipeline: first during classification inference in the computer vision model, and then again as a post-processing step for the model's classifications. While developing this approach, we ask two primary questions: (1) How does error in DNA metabarcoding data affect the accuracy of the computer vision classification model? (2) What are the strengths and limitations of different taxonomic granularity refinement methods? In addition to the case study we present here, we have also developed a GitHub repository to allow this framework to easily be adapted to other study systems (Blair, 2024).

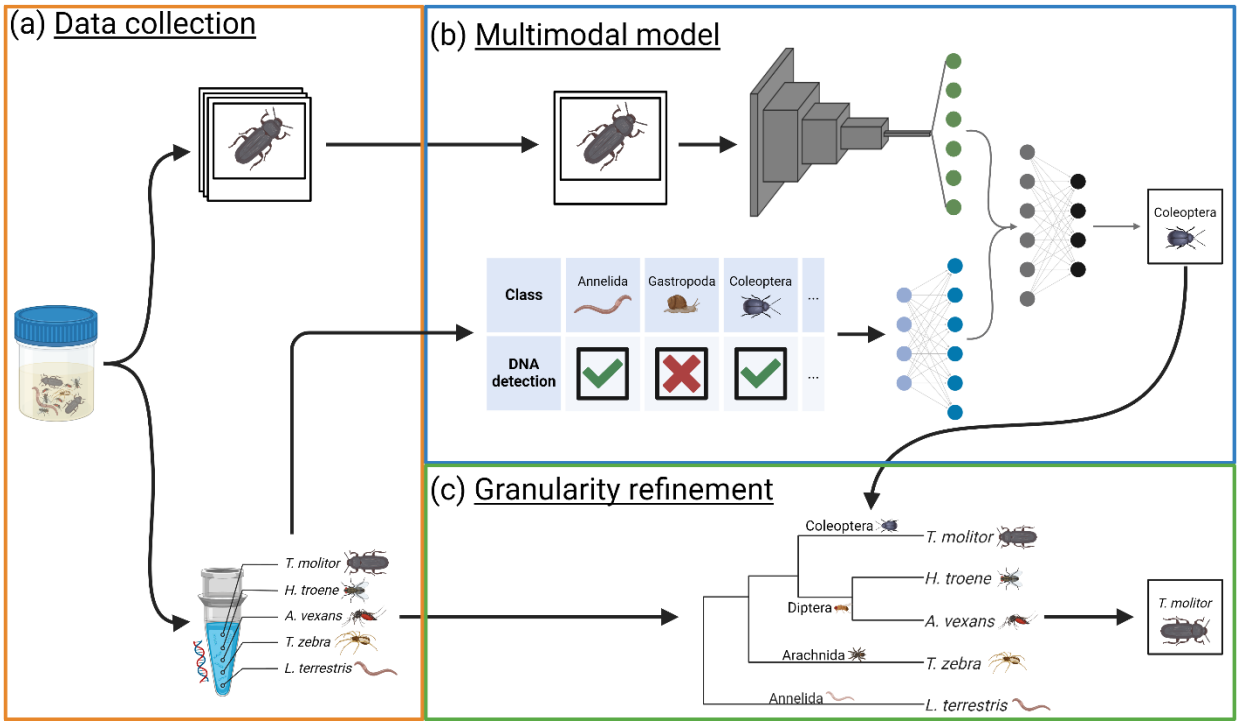


Figure 1: Our framework for combining computer vision and DNA metabarcoding to improve the accuracy and taxonomic granularity of classifications. (a) Images and DNA metabarcoding data are collected concurrently from bulk samples. (b) Images and DNA assemblage data are used as input for a multimodal classification model. The features of the image input are extracted using a convolutional neural network. The DNA assemblage data provides presence/absence information for the model's known classes and is input as a binary vector into a dense neural network. The image features and the DNA features are concatenated and processed to produce a final classification. (c) By interpreting the DNA metabarcoding detections hierarchically and cross-referencing them with the model's classifications, the taxonomic granularity of the classifications can be refined.

## 2. Methods

### 2.1 Data collection

#### 2.1.1 Specimen collection

Each year, the National Ecological Observatory Network (NEON) performs standardized pitfall trap array sampling across the United States, including Alaska, Hawaii, and Puerto Rico (Hoekman et al. 2017). The focal taxa of the pitfall trap array project are ground beetles (Coleoptera: Carabidae), which are collected, identified, and counted by NEON staff members

once every two weeks during the growing season (defined as “the weeks when average minimum temperatures exceed 4 ℃ for 10 days and ending when temperatures remain below 4 ℃ for the same period”, Kaspari et al., 2022). The remaining pitfall trap contents are set aside as ‘Invertebrate Bycatch’ and archived in 95% ethanol-filled 50 mL falcon tubes. Hereon, a single collection period from a pitfall trap plot is referred to as a “sampling event”.

The invertebrate bycatch specimens used in this research were taken from 56 NEON trap plots from 27 sites (usually two plots per site; Figure 2, Figure S.1). Generally, we used three sampling events per plot, selected at the beginning, middle, and end of each site's growing season. This resulted in a total of 150 sampling events. All sampling events used here were collected in 2016 and processed in 2019. The focus of this project was to classify the invertebrate bycatch, so ground beetles and non-invertebrate specimens were not considered.

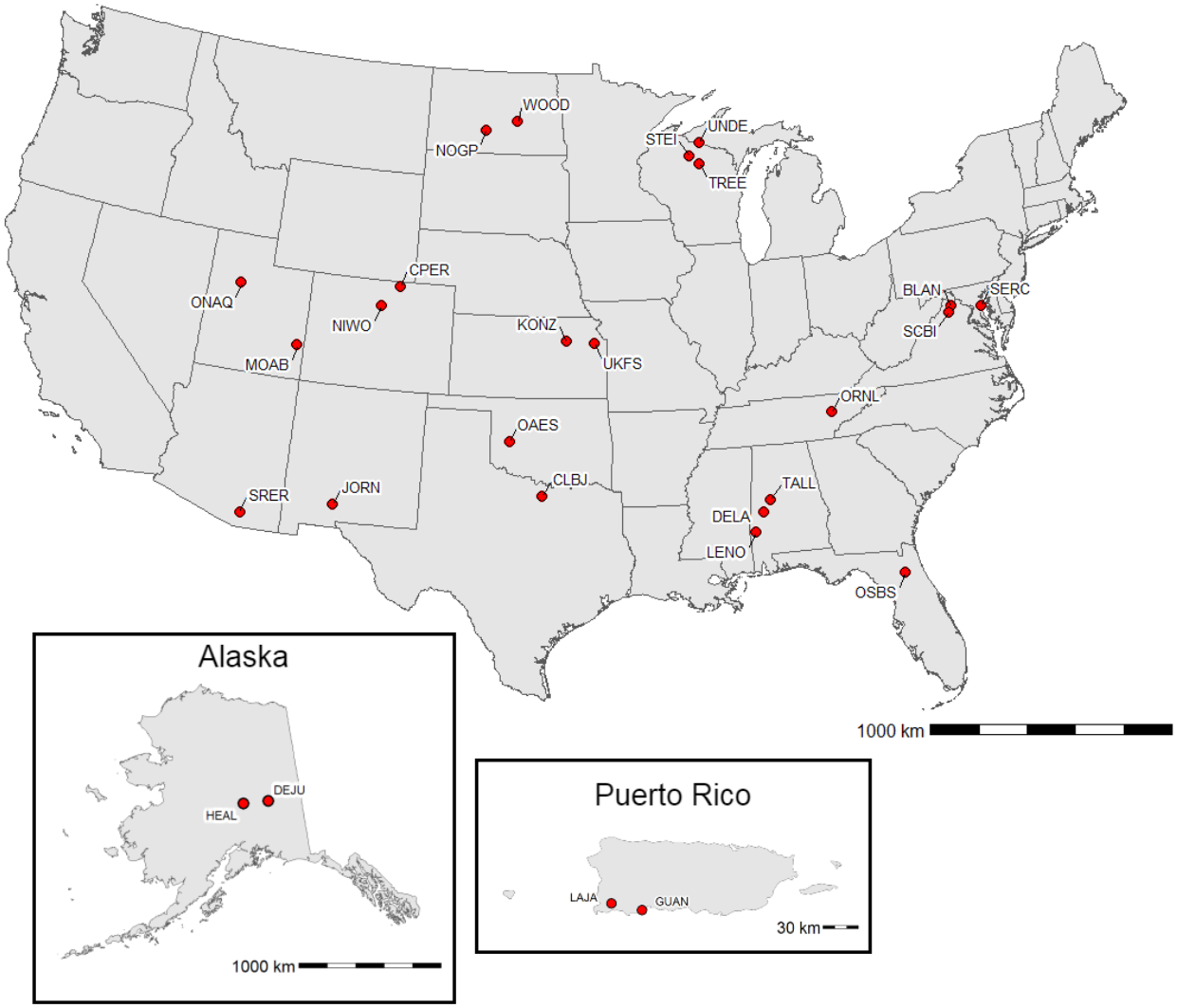


Figure 2: Map of the 27 NEON sampling sites used in this study. The sites are labelled with their abbreviated names.

2.1.2 Imaging

The contents of each 50mL falcon tube were spread out across a 20.32 cm ✕ 30.48 cm (8” ✕ 12”) white ceramic tile and photographed at a resolution of 729 pixels per $mm^2$, as described by Weiser et al., 2021 (Figure S.2). Using the FIJI implementation of ImageJ (Schindelin et al., 2012), each specimen was detected and cropped to its bounding box to produce a final image.

2.1.3 DNA extraction and metabarcoding

The DNA metabarcoding data used in this study was collected for Weiser et al., 2022, which used the same sampling events described in Section 0. In brief, DNA metabarcoding was conducted on a per-tube basis (Figure S.1). Ethanol from each falcon tube was filtered individually (i.e., one filter per tube) and DNA was extracted from the filters using established protocols (Weiser et al., 2022). The cytochrome c oxidase I (COI) barcode region (141-254 base pairs) was then amplified using a two-step polymerase chain reaction (PCR) protocol and sequenced on an Illumina MiSeq. Three COI primers were used: 157, LCO, and Lep (Rennstam Rubbmark et al., 2018; Hajibabaei et al., 2019; Weiser et al., 2022). Sequences were clustered into Operational Taxonomic Units (OTUs) and each OTU was assigned a taxonomic classification using NCBI BLASTn (Altschul *et al.*, 1990) and Integrated Taxonomic Information System (ITIS) (U.S. Geological Survey, 2013). Only sequences with ≥ 97% similarity between the OTU consensus sequence and the BLASTn search were used. See Weiser et al., 2022 for the full DNA extraction and metabarcoding methods.

In total, across all sampling events, there were 10,212 DNA metabarcoding detections. To align the DNA data with the imaging data, we removed any DNA detections from sampling events not included in the image dataset, as well as duplicate detections (i.e. multiple detections of the same taxon in a single sampling event, for example due to amplification using multiple primers). This yielded a final DNA metabarcoding dataset with 3,361 detections and 1,212 unique taxa, primarily consisting of family (369 detections; 85 unique), genus (468 detections; 183 unique), and species-level (2,471 detections; 922 unique) detections.

## 2.2 Data and labelling

### 2.2.1 Computer vision class labels

The taxonomic scope of the image and DNA metabarcoding data spanned three invertebrate phyla: Annelida, Arthropoda, and Mollusca. The specimen images were labelled by a single technician to the best of their ability (as described in Blair *et al.*, 2022). The final labels used for our study ranged from order to phylum-level. Classes with a taxonomic granularity coarser than order-level but with no subtaxa present in the dataset (e.g. Phylum: Annelida) were included. Specimens labelled as nested classes at a taxonomic granularity coarser than order-level (Phylum: Arthropoda, Class: Insecta, and Class: Arachnida) were excluded. Classes with fewer than 100 specimens in the dataset were also excluded. This resulted in a final image dataset with a total of 36,988 specimens across 17 classes (13 orders and one subclass, class, subphylum, and phylum; Figure 3).

Figure 3: Collage of photographs of all invertebrate classes used in the training dataset (n = 17). The taxonomic granularity of the classes ranges from order to phylum. Specimens were cropped from their original photographs, and the background was removed. Relative scale of each specimen is conserved.

### 2.2.2 Hierarchical labels

Hierarchical labels containing taxonomic information at multiple levels and were assigned to images and sampling events. Image-based hierarchical labels contained information at six levels from phylum to order-level for individual specimens (Table 1). DNA-based hierarchical labels contained information at 13 levels from phylum to species for all DNA detection in each sampling event (Table 2). The levels in the DNA-based hierarchical labels were phylum, subphylum, class, subclass, superorder, order, suborder, infraorder, superfamily, family, subfamily, genus, and species. We used these labels as part of the taxonomic granularity improvement process detailed in Section 2.5.

Table 1: Three examples image-based hierarchical labels (a,b,c). (a) The hierarchical label for Blattodea with all taxonomic levels between phylum and order filled. (b) Some taxa do not have names for every taxonomic sub-level. In these cases, the name from the preceding, finer-grain level is used. In this example, Coleoptera does not belong to any superorder, so "Coleoptera" is used as a placeholder superorder name. (c) Classes with a taxonomic granularity above order-level used indeterminate ("indet.") labels at all remaining taxonomic levels. In this example, "Annelida indet." is used for all levels below phylum.

| Example | Phylum | Subphylum | Class | Subclass | Superorder | Order |
|---|---|---|---|---|---|---|
| (a) | Arthropoda | Hexapoda | Insecta | Pterygota | Polyneuroptera | Blattodea |
| (b) | Arthropoda | Hexapoda | Insecta | Pterygota | *Coleoptera* | Coleoptera |
| (c) | Annelida | *Annelida indet.* | *Annelida indet.* | *Annelida indet.* | *Annelida indet.* | *Annelida indet.* |

Table 2: Simplified example of a DNA multi-class hierarchical label for a sampling event. Our DNA hierarchical labels used 13 taxonomic levels from phylum to species, but for the sake of space only major taxonomic levels are shown here.

| Phylum | Class | Order | Family | Genus | Species |
|---|---|---|---|---|---|
| Arthropoda | Insecta | Diptera | Culicidae | *Aedes* | *A. vexans* |
| | | | | *Culex* | *C. salinarius* |
| | | Orthoptera | Gryllidae | *Gryllus* | *G. veletis* |
| | Arachnida | Araneae | Lycosidae | *Schizocosa* | *S. humilis* |

2.2.3 Binary assemblage data

Two sets of binary assemblage data were recorded for each sampling event: one using detections from the image labels and one using detections from the DNA class labels. DNA class labels were based on the same 17 classes used by the computer vision model, and followed the same naming scheme described in Section 0. The assemblage data was multi-hot encoded (Goodfellow, Yoshua and Courville, 2016). That is, each sampling event was assigned a 17 element long binary vector where each element corresponded to a computer vision class. If the class was detected in the sampling event, its element was assigned a score of 1, whereas it was assigned a score of 0 if it was not detected. This data was used as input for some classification models described in Section 0.

## 2.3 Training and testing data split

Quasi-replication occurs in machine learning datasets when the same or very similar data occur in both the training and testing datasets. This violates the assumption of independence between training and testing data and should be avoided to make valid inferences on the test data. The

DNA-based assemblage data presented a quasi-replication risk, as specimens from the same sampling event would have the same assemblage data. To avoid quasi-replication, we split the training and testing such that all specimens from a given sampling event were only included in either the training or testing data. We set our target training:testing ratio to 85:15, and we randomly added sampling events to the test dataset until the test dataset contained >15% of the total number of specimens. The final train:test split was 31,381: 5,617 specimens and 122:28 sampling events.

## 2.4 Classification models

The objective of all the classification models was to accurately classify the class labels of individual specimen photos. Classification masks (Section 0) and data fusion approaches (Section 0) were used to assess how classification accuracy changes when DNA-based assemblage data was added to the specimen classification pipeline. Performance of each classification model was assessed using the original image labels as a ground truth. All code required for running these models can be found in the "Model_Scripts" subdirectory of our GitHub repository (Blair, 2024).

### 2.4.1 Baseline model

To evaluate model performance in the absence of DNA-based assemblage data, we trained a ResNet-50 (He et al., 2016) as a baseline model using only image data. The model was pre-trained using the ImageNet weights from He et al. (2016), and then fine-tuned using the NEON invertebrate bycatch image data. The ImageNet classification layer was removed and replaced with a new classification layer for our 17 classes.

### 2.4.2 Classification masks

#### *2.4.2.1 Naïve mask*

For our first experiment in combining the image and DNA-based assemblage data, we used what we call a "naïve mask" on the baseline model's test data softmax classification layer outputs. Using the naïve mask, the softmax layer values for each test data specimen were multiplied by their sampling event's binary DNA-based assemblage data. Thus, any classes not detected by the DNA metabarcoding in a given sampling event had their respective softmax values set to 0, whereas the remaining classes were unaffected. After applying the mask, the class label with the highest softmax value was used as the classification for a given specimen.

#### *2.4.2.2 Weighted mask*

"Hard" masks like the naïve mask, which set the softmax values of undetected classes to 0, assume the DNA metabarcoding data is error-free. However, in reality, DNA metabarcoding can have false positive and/or false negative detections (Taberlet *et al.*, 2018). To create a "softer" version of the naïve mask, we also created a "weighted mask", which allows classes not detected by the DNA metabarcoding to still be classified.

The weights for the weighted mask were calculated using the DNA's true positive rate (precision) and false negative rate (1 - recall) for each class. The DNA metabarcoding precision and recall were calculated by comparing the DNA-based assemblage labels to the image-based assemblage labels, using the image-based assemblage labels as a ground truth. To create the weighted mask, we assigned a class's precision for positive DNA detections, and the class's false negative rate for negative detections. The application of the weighted mask was the same as the

naïve mask: The softmax values for each test data specimen were multiplied by their sampling event's weighted mask values, and the new top-1 class was used as the classification.

*2.4.2.3 Image-based mask*

To simulate a scenario where the DNA detections were in perfect alignment with the image-based detections, we applied the image-based binary assemblage data to the softmax values of the baseline model. We did this to provide an upper-bound for the classification mask accuracy, and to understand how DNA detection accuracy impacts specimen classification accuracy when using classification masks.

2.4.3 Multimodal fusion

To allow the classification models to learn patterns from the DNA data, we trained multimodal models that combined images with binary DNA-based assemblage data using intermediate fusion (Boulahia *et al.*, 2021) (Figure 4). In these multimodal models, the image and assemblage data for a given specimen were fed to the model separately. The images were fed through the ResNet-50 architecture, ultimately producing a flat feature layer. DNA-based assemblage data was paired with individual specimens based on their sampling event (the same approach as the classification masks described in Section 2.4.2). This data is fed through a single fully-connected layer. The flattened image layer and fully-connected DNA-based assemblage layer were then concatenated (i.e. fused) and passed through another fully-connected layer before reaching the final classification layer.

To understand the effect that DNA detection accuracy has on classification performance, we ran three versions of the multimodal model using different types of assemblage data as input: (1)

using the DNA-based assemblage data, (2) using the image-based assemblage data, and (3) using 'zero-filled' assemblage data (all values in the assemblage data are set to zero). In all three experiments the training and testing datasets used the same assemblage data type (i.e. DNA-based, image-based, or zero-filled). All three experiments used the same overall model architecture as described in Figure 4. The purpose of the image-based assemblage experiment was to simulate the results of a model where the DNA detections perfectly aligned with the ground truth labels. The purpose of the zero-filled assemblage experiment was to control for differences in model architecture when comparing the multimodal models to models trained without DNA-based assemblage data, as the zero-filled data would provide no informative value to the model. The zero-filled assemblage data had the same dimensions as the other assemblage data (17 values for each sampling event).

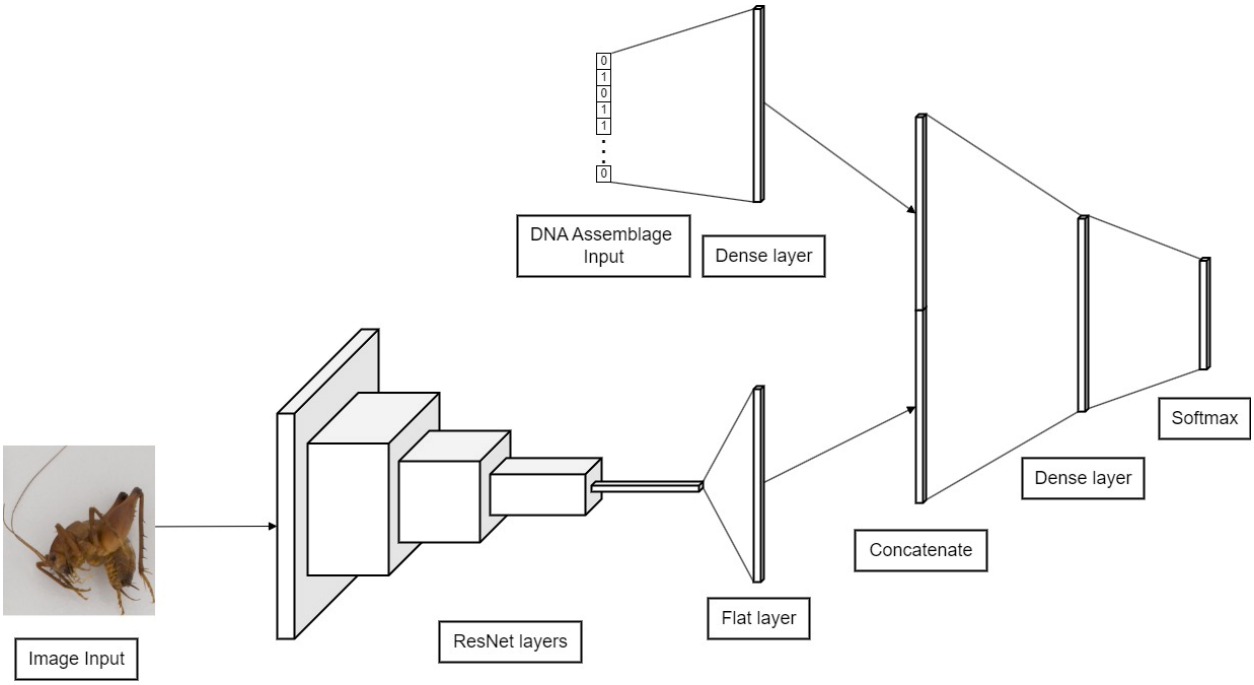


Figure 4: The described classification model architecture that combines image data with DNA-based binary assemblage data. Images are fed through ResNet convolutional layers to produce a flat feature layer, and DNA assemblage data produces a fully connected dense layer. The flat layer and dense layer are then concatenated and passed through one more dense layer before final classification in the softmax

layer. The visual proportions of each layer have been simplified to ease interpretation and are not meant to be interpreted as 1:1 representations of the exact layer sizes.

### 2.5 Refining taxonomic granularity using DNA-based assemblage data

To take advantage of the relatively fine taxonomic granularity of the raw DNA detections compared to the computer vision classes, we refined the taxonomic granularity of the DNA fusion model classifications by cross-referencing them with the DNA detections. In cases where the model classifications and DNA detections agreed on the presence of a class, the granularity of the classification improved until the number of subtaxa detected by the DNA metabarcoding was greater than 1 or the granularity reached species-level, as that was the finest granularity reported by the DNA (Figure 5a,b). In cases where the model classifications and DNA detections disagreed on the presence of the class classified by the model, we implemented two methods which we call “model-biased” and “DNA-biased”. The model-biased method is simple. In cases where the model and DNA metabarcoding disagreed, the model classification remained unchanged (Figure 5c). When using the DNA-biased method, we compared the hierarchical label of the classified specimen to the hierarchical labels of the sampling event as determined by the DNA metabarcoding (Figure 5d, Table 1,

Table **2**). Starting from the original classification level, we coarsened the granularity of the label until an agreement between the model and DNA metabarcoding was reached. The taxonomic name at this level became an intermediate label, and the taxonomic granularity of the label was refined until the number of subtaxa detected by the DNA metabarcoding was greater than 1 or the granularity reached species-level.

All code required for running these methods can be found in the "Granularity_Refinement" subdirectory of our GitHub repository (Blair, 2024).

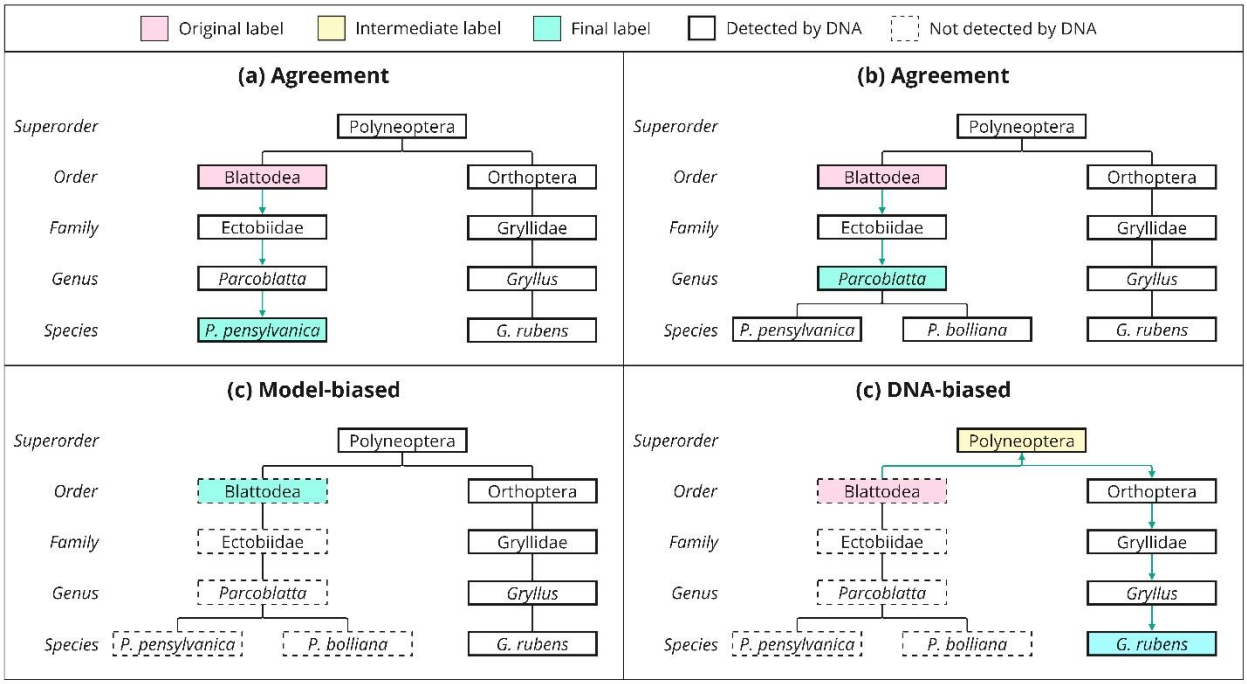


Figure 5: Four methods of changing a label's granularity using DNA detections. (a,b) When the classification label and DNA detections are in agreement about the presence of a class, granularity will be refined until the number of subtaxa detected by the DNA metabarcoding is > 1 or the classification reaches species level. (c) Under the model-biased approach, when the classification label and DNA metabarcoding do not agree on the presence of a class, the classification label remains unchanged. (d) Under the DNA-biased approach, when the classification label and DNA metabarcoding do not agree on the presence of a class, the granularity of the classification label is coarsened until a DNA detection for the class is found ("intermediate label"). The granularity of the intermediate label is then refined using the same rules as (a,b).

## 3. Results

### 3.1 DNA metabarcoding precision and recall

To generate the weights for the weighted mask, we calculated the DNA-based assemblage data's precision and recall for each class using the image-based assemblage data as the ground truth. This calculation only included sampling events from the training dataset. Across the 17 predicted classes, recall ranged from 0.905 to 0.000, with an average recall of 0.570. The weight for a negative detection was 1 - recall, so negative detection weights ranged from 1.000 to 0.095, with an average of 0.430. Two classes (Opilioacarida and Zygentoma) were never detected by the DNA. Across the 15 classes detected by the DNA, the average precision was 0.761. The precision and recall values per class are reported in Table S.1.

### 3.2 Classification accuracy

Compared to the baseline model, the DNA assemblage fusion model improved accuracy by 2.2% (79.6% vs 77.4%; Table 3). However, the DNA assemblage fusion model's accuracy was 1.0% lower than the zero-filled model's accuracy (80.6%). This suggests that some of the performance improvements seen in the fusion models could come from changes to the model architecture. The naïve classification mask recorded the lowest classification metrics, with an accuracy 22.6% below the baseline model (54.8%), and a top-3 accuracy of only 64.0%.

Experiments with image-based assemblage data performed better, with the fusion model reaching an average accuracy of 83.6% and a balanced accuracy (i.e. macro-averaged recall) of 0.713 (Table 4). The image-based naive mask accuracy was 25.8% better than the DNA-based

naive mask, and 3.2% better than the baseline model. It also had the highest top-3 accuracy across all experiments at 93.2%.

Table 3: Performance metrics for experiments trained using DNA-based assemblage data, other than the baseline model, which was trained only using images, and the 'zero-filled' experiment, which replaced all assemblage data values with zero to control for the impact of model architecture. Underlined scores indicate they are the highest for a given metric.

| Experiment | Accuracy | Balanced Accuracy | Top-3 Accuracy |
|---|---|---|---|
| **Baseline** | 0.774 | 0.674 | 0.952 |
| **Naive mask** | 0.548 | 0.509 | 0.640 |
| **Weighted mask** | 0.764 | 0.666 | 0.950 |
| **Fusion (DNA)** | 0.796 | <u>0.680</u> | <u>0.957</u> |
| **Fusion (zero-filled)** | <u>0.806</u> | 0.670 | 0.952 |

Table 4: Performance metrics for the image-based assemblage data experiments. These experiments used binary assemblage data taken from the ground truth specimen labels. Underlined scores indicate they are the highest for a given metric.

| Experiment | Accuracy | Balanced Accuracy | Top-3 Accuracy |
|---|---|---|---|
| **Mask** | 0.806 | 0.690 | 0.959 |
| **Fusion** | <u>0.836</u> | <u>0.713</u> | <u>0.963</u> |

### 3.3 Taxonomic granularity

Of the DNA fusion model classifications, 68.2% (3833/5617) were present in their corresponding sampling event's DNA assemblage data. Nonetheless, both approaches for handling disagreements between the DNA and classification model (model-biased or DNA-biased) improved the average taxonomic granularity of the classifications (Figure 6). Despite starting with no classifications finer than order-level, the DNA-biased approach resulted in 5.7% of classifications improving to species-level and the model-biased approach resulted in 5.1% of the classifications improving to species-level. The DNA-biased approach was more effective

overall at refining the granularity of classifications, with 72.2% of classifications becoming finer than their original classification, and 43.1% reaching at least family-level. In the model-biased approach, 51.7% of classifications improved their granularity, and 31.0% reached family-level or lower. When looking exclusively at classifications where the DNA assemblage data and fusion model classifications agreed on the presence of a class, 7.5% reached species level, 45.4% reached family-level or lower, and 75.7% became finer than their original classifications. Both the DNA-biased and model-biased approaches produced 89 unique final labels (Table S2).

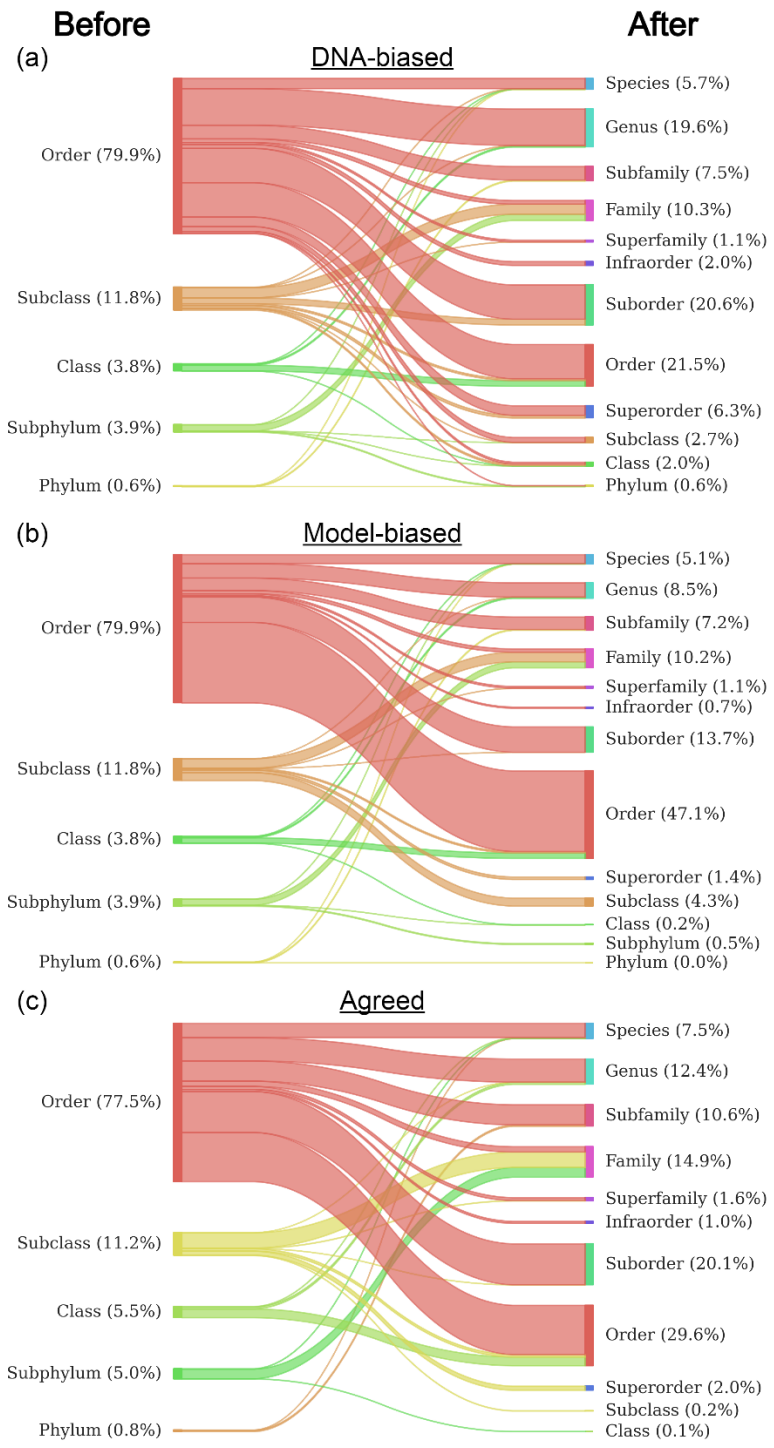


Figure 6: Sankey diagrams showing the change in taxonomic granularity before (left) and after (right) cross-referencing labels with the DNA detections. (a) DNA-biased approach. (b) Model-biased approach. (c) Results when the model classification and DNA detections agree on the presence of the labelled class.

## 4 Discussion

Here we show that combining concurrent DNA-based assemblage data with computer vision can improve the accuracy and taxonomic granularity of computer vision classifications. Unlike most classification pipeline enhancements which only focus on improving the ability to classify classes on which it was trained ("known classes"), this approach adds the ability for the pipeline to infer classifications beyond the model's usual taxonomic scope ("unknown classes"). To thoroughly explore the benefits and implications of this hybrid approach, we focused on the following two research questions.

### 4.1 How does DNA metabarcoding accuracy affect specimen classification accuracy?

The effect of metabarcoding accuracy on classification accuracy differed between the classification masks and the multimodal fusion models, illuminating a key difference between them: classification masks (as used in this study) do not take class co-occurrence into consideration, whereas the multimodal models do. Put another way, in a classification mask the only factor that directly influences the weight given to a class is the presence or absence of the class itself. Conversely, the neural networks of multimodal fusion models—with their fully-connected structure—allow the presence or absence of all classes to holistically influence each class's classification probability. This allows the model to use patterns of class co-occurrence to inform its classification decisions.

The different mechanisms used by classification masks and multimodal models are best demonstrated in Table 4, where the assemblage data was derived from the ground-truth image labels. In the classification mask, the model's original classifications were exclusively based on image data, and any classifications that did not match their respective assemblage data were

reclassified as the class with the highest softmax score that was present in the specimen's assemblage. Given that the assemblage data was derived from the ground truth labels, this mask acted as a sieve that filtered out any classes that could not possibly be the correct classification based on the assemblage data. As a result, it could only have a positive impact on accuracy. However, despite this, the fusion model still scored higher on all three metrics measured (top-1 accuracy, balanced accuracy, and top-3 accuracy). This implies that the fusion model was not just using the assemblage data as a filter, but that it provided additional contextual information (such as class co-occurrence or class exclusion) that further improved accuracy. Thus, due to the fusion model's ability to holistically evaluate occurrence data, and as illustrated through its superior performance compared to classification masks even under ideal conditions, multimodal fusion models are likely to be preferable in most use cases. This conclusion is reinforced by the results of Table 3, where both naïve and weighted masks showed negative effects on all classification performance metrics when the DNA-based assemblage data contained substantial amounts of error.

### 4.2 What are the strengths and limitations of each granularity refinement method?

Here we proposed two approaches for cross-referencing DNA metabarcoding data to achieve the novel ability of refining the taxonomic granularity of computer vision classifications. The two approaches differ in how they resolve disagreements between the detections of the DNA metabarcoding and computer vision classifications, with the model-biased approach favouring the computer vision classifications, and the DNA-biased approach favouring the DNA detections. As such, each approach has its own set of advantages and limitations.

Through the ability to coarsen granularity before refining it, the DNA-biased method can make classifications outside of the taxonomy of the original classification model (Figure S.3). Explained another way, the model-biased approach and traditional hierarchical classifiers (e.g. Badirli *et al.*, 2023) can only adjust classifications "vertically" (i.e. to supertaxa or subtaxa of the original classifications), but the DNA-biased approach can also adjust classifications "laterally" to out-of-distribution taxa through a combination of classification coarsening and refining. Classification of out-of-distribution taxa is usually only possible using feature embedding learning methods such as zero-shot learning (Badirli *et al.*, 2021). An illustrative example of this comes from the DNA-biased approach's detection of taxa within the insect order Psocodea (e.g. *Valenzuela flavidus*; Table S.2). As Psocodea was not included as a class in our model, and our model's finest taxonomic granularity was order-level, Psocodea's branch of the taxonomy was only accessible through a "lateral" taxonomic adjustment (Figure S.3). As such, it was only detected by the DNA-biased approach, and not the model-biased approach (Table S.2). In theory, this extends the range of possible classifications to the full taxonomic scope of the genetic reference database being used (e.g. GenBank, Barcode of Life, etc.) (Ratnasingham and Hebert, 2007; Sayers *et al.*, 2024). In practice, it is likely best to self-impose limits on how much the DNA-biased method can coarsen granularity. In our case we limited ourselves to phylum, as we were only interested in classifications within our three focal phyla.

While it does not have the same potential taxonomic scope of the DNA-biased approach, an advantage of the model-biased approach is that the taxonomic granularity of the final classification cannot be coarser than the original classification. Applied to the DNA fusion model classifications, 9.9% of all classifications became coarser when the DNA-biased method was used (Figure 6). While the DNA-biased method classified more specimens at family-level or

finer (43.1% vs 31.0%), the ability to coarsen granularity resulted in more classifications above order-level (11.7% vs 6.4%).

Even when granularity does not reach species, classifications that match with the DNA-based assemblage data still provide more information than what is typically output from a classification model. This is because we can also see the number and identity of subtaxa that the specimen could be according to the DNA metabarcoding detections. For example, if the DNA metabarcoding detected three species of the cricket genus *Gryllus* in a sample, we could say the label of a specimen that would otherwise be classified simply as "*Gryllus* indet." is actually one of three possible species of *Gryllus*, as detected by the DNA metabarcoding (e.g. *G. pennsylvanicus*, *G. rubens*, or *G. veletis*). This might also be useful for future developments to these methods, as the number of subtaxa detected by the DNA metabarcoding could be used to inform clustering algorithms that separate the specimens into morphotaxa.

Of course, the granularity of classifications matters little if they are not accurate. A caveat of our study is that we cannot verify the accuracy of granularity-refined classifications, as they are at lower taxonomic levels than our ground truth (human-classified) labels. However, we know that our classification models were more accurate than the DNA assemblage data when compared to our ground-truth labels. Thus, the DNA-biased method of refining granularity will likely add more error to the classifications than the model-biased approach. When deciding between the two methods, this is likely to be a determining factor: does the computer vision model or DNA metabarcoding contain more error?

### 4.3 Caveats and areas for future exploration

In an applied context, we cannot definitively conclude that image-DNA fusion models as we present here improve specimen classification accuracy. This is primarily due to the high rates of disagreement (or "error") between our DNA metabarcoding detections and image-based detections. When comparing our three fusion experiments, the zero-filled experiment had a top-1 accuracy 1.0% higher than the DNA-based assemblage data experiment, but 3.0% less than the image-based assemblage data experiment. This suggests that in an ideal situation where the DNA-based assemblage data has low amounts of error (i.e. it is more similar to the image-based assemblage data), image-DNA fusion models will positively impact classification accuracy. However, when the DNA-based assemblage data contains substantial error, differences in performance between the baseline and fusion models likely arise from changes in the model's architecture.

Reconciling genetic-based and morphology-based data—the two chief methods for invertebrate biodiversity monitoring—is a pressing need as previous studies have shown that assemblages determined by visual classification usually differ from assemblages determined using DNA metabarcoding. For example, Emmons *et al.* (2023) found that NEON benthic macroinvertebrate samples classified by taxonomists only shared 59% of order-level detections with DNA metabarcoding data derived from homogenized blends of the same samples. Marquina *et al.* (2019) also found that different DNA sampling protocols can produce inconsistent assemblage data, as DNA metabarcoded from ethanol vs homogenized blends of the same samples yielded significantly different assemblage data, with both methods detecting taxa not detected by the other. For the image-DNA fusion methods we propose here to be maximally effective, advances

will need to be made in DNA metabarcoding methodology to limit false positive and false negative detections.

Beyond DNA metabarcoding accuracy, there are likely other factors that can impact the efficacy of our methods, such as assemblage homogeneity and assemblage specificity. Assemblage homogeneity refers to the variation among assemblages. For example, the zero-filled assemblage experiment used data that was completely homogenous, as every sampling event had the same assemblage data. Assemblage specificity refers to how many unique classes are detected within a sample. A maximally specific assemblage would only detect one class as present, while a minimally specific assemblage would detect every class as present. Reducing assemblage homogeneity and increasing assemblage specificity should yield models with greater classification performance. This is because heterogeneity is required for learnable patterns to emerge in the data, and increased specificity allows more classes to be filtered out by the model. This is partially demonstrated by comparing the results of Blair *et al.* (2020) to the results we present here. In their study, which built classification models for NEON's carabid beetles, the authors applied classification masks to their models based on the detected ground beetle assemblages at each sampling site. On average, 2.93 out of 25 potential species (11.7%) were detected per site, resulting in an accuracy improvement of 10.9% (84.7% → 95.6%) after applying the classification masks. Comparatively, our image-based assemblages detected an average of 9.09 out of 17 potential classes (53.5%) per sampling event. When compared to the baseline model, this resulted in an accuracy improvement of 3.2% when using the classification mask and 6.2% in the fusion model (Table 3, Table 4). Thus, methods to reduce assemblage homogeneity (e.g. finer-grain class labels) and increase assemblage specificity (e.g. fewer

specimens per sample) will likely increase the efficacy of image-DNA metabarcoding fusion classification pipelines.

### 4.4 Broader applications and implications

In this study, we used assemblage data derived from DNA metabarcoding to improve computer vision classifications of terrestrial invertebrates. However, our general framework could be applied to any study system where images and DNA metabarcoding data are collected concurrently. Given that computer vision and DNA metabarcoding are emerging technologies in ecological research, the number of research systems that include one or both is increasing (Pichler and Hartig, 2023; Shea *et al.*, 2023). Projects that use both computer vision and DNA metabarcoding also span a wide range of fauna and ecosystems, including freshwater, marine, and terrestrial vertebrates (Takeuchi *et al.*, 2021; Mas-Carrió *et al.*, 2022; Holm *et al.*, 2023). By leveraging the strengths of computer vision and DNA metabarcoding, our framework could enhance the capabilities of projects like these.

Our framework is composed of two primary modules—a multimodal classification model and a classification granularity refinement method—which can be used and modified independently of each other. Our multimodal model requires image data and assemblage data, but the assemblage data does not need to be derived from DNA. In this study we conducted experiments where the DNA-derived assemblage data was substituted with image-derived assemblage data. Likewise, assemblages derived from other sensor data (acoustic, lidar, etc.) could also be used (Gasc *et al.*, 2015; Kaplan *et al.*, 2015; Wedding *et al.*, 2019). Conversely, our classification granularity refinement method requires DNA metabarcoding data and individual specimen classifications, but the specimen classifications do not need to be derived from a computer vision model. We

encourage future studies to explore different variations and combinations of the modules we present here.

Our framework's ability to refine classification granularity, which is typically not possible in computer vision, could improve the feasibility of building broad-scope, fine-grain classification models (e.g. models spanning entire classes or phyla and capable of producing species-level classifications). This typically requires vast amounts of training data, as training examples need to be provided for every species. Using the approach that we present here, classifiers could be trained at coarser taxonomic levels such as order or family and still have the potential to produce species-level classifications. This would decrease the number of classes in the model, and thus data needed to train it, by orders of magnitude. Hence, the synergy between DNA metabarcoding and computer vision outlined in this study paves the way for new possibilities in computer vision classification of taxa, with the potential for improved accuracy and granularity with far less data dependency.

## References


Altschul, S.F. *et al.* (1990) 'Basic local alignment search tool', *Journal of Molecular Biology*, 215(3), 403–410. https://doi.org/10.1016/S0022-2836(05)80360-2.

Ärje, J. *et al.* (2020) 'Automatic image-based identification and biomass estimation of invertebrates', *Methods in Ecology and Evolution*, 11(8), 922–931. https://doi.org/10.1111/2041-210X.13428.

Badirli, S. *et al.* (2021) 'Fine-Grained Zero-Shot Learning with DNA as Side Information', in *Advances in Neural Information Processing Systems*. Curran Associates, Inc., 19352–19362. https://proceedings.neurips.cc/paper_files/paper/2021/hash/a18630ab1c3b9f14454cf70dc7114834-Abstract.html (Accessed: 24 July 2024).

Badirli, S. *et al.* (2023) 'Classifying the unknown: Insect identification with deep hierarchical Bayesian learning', *Methods in Ecology and Evolution*, 14(6), 1515–1530. https://doi.org/10.1111/2041-210X.14104.

Beery, S. *et al.* (2020) 'Synthetic examples improve generalization for rare classes', in *Proceedings - 2020 IEEE Winter Conference on Applications of Computer Vision, WACV 2020*. https://doi.org/10.1109/WACV45572.2020.9093570.

Beery, S., Van Horn, G. and Perona, P. (2018) 'Recognition in Terra Incognita', in *Lecture Notes in Computer Science (including subseries Lecture Notes in Artificial Intelligence and Lecture Notes in Bioinformatics)*. https://doi.org/10.1007/978-3-030-01270-0_28.

Berg, T. *et al.* (2014) 'Birdsnap: Large-scale fine-grained visual categorization of birds', in *Proceedings of the IEEE Computer Society Conference on Computer Vision and Pattern Recognition*, 2011–2018. https://doi.org/10.1109/CVPR.2014.259.

Bista, I. *et al.* (2018) 'Performance of amplicon and shotgun sequencing for accurate biomass estimation in invertebrate community samples', *Molecular Ecology Resources*, 18(5), 1020–1034. https://doi.org/10.1111/1755-0998.12888.

Blair, J.D. *et al.* (2020) 'Robust and simplified machine learning identification of pitfall trap-collected ground beetles at the continental scale', *Ecology and Evolution*, 10(23), 13143–13153. https://doi.org/10.1002/ece3.6905.

Blair, J.D. *et al.* (2022) 'Embracing imperfection: Machine-assisted invertebrate classification in real-world datasets', *Ecological Informatics*, 72, p. 101896. https://doi.org/10.1016/j.ecoinf.2022.101896.

Blair, J.D. (2024) 'CV-DNA-Hybrid'. Zenodo. https://doi.org/10.5281/ZENODO.13621526.

Boulahia, S.Y. *et al.* (2021) 'Early, intermediate and late fusion strategies for robust deep learning-based multimodal action recognition', *Machine Vision and Applications*, 32(6), p. 121. https://doi.org/10.1007/s00138-021-01249-8.

Deiner, K. *et al.* (2017) ‘Environmental DNA metabarcoding: Transforming how we survey animal and plant communities’, *Molecular Ecology*, 26(21), 5872–5895. https://doi.org/10.1111/mec.14350.

Emmons, S.C. *et al.* (2023) ‘DNA metabarcoding captures different macroinvertebrate biodiversity than morphological identification approaches across a continental scale’, *Environmental DNA*, p. edn3.453. https://doi.org/10.1002/edn3.453.

Friedland, G. (2024) *Information-Driven Machine Learning: Data Science as an Engineering Discipline*. 1st ed. Cham: Springer International Publishing AG.

Gasc, A. *et al.* (2015) ‘Acoustic indices for biodiversity assessments: Analyses of bias based on simulated bird assemblages and recommendations for field surveys’, *Biological Conservation*, 191, 306–312. https://doi.org/10.1016/j.biocon.2015.06.018.

Goodfellow, I., Yoshua, B. and Courville, A. (2016) *Deep Learning*. Cambridge: The MIT Press.

Guillera-Arroita, G. *et al.* (2017) ‘Dealing with false-positive and false-negative errors about species occurrence at multiple levels’, *Methods in Ecology and Evolution*. Edited by R. McCrea, 8(9), 1081–1091. https://doi.org/10.1111/2041-210X.12743.

Hajibabaei, M. *et al.* (2019) ‘COI metabarcoding primer choice affects richness and recovery of indicator taxa in freshwater systems’, *PLOS ONE*. Edited by A. Ramaiah, 14(9), p. e0220953. https://doi.org/10.1371/journal.pone.0220953.

He, K. *et al.* (2016) ‘Deep residual learning for image recognition’, in *Proceedings of the IEEE Computer Society Conference on Computer Vision and Pattern Recognition*. https://doi.org/10.1109/CVPR.2016.90.

Holm, A.M.R. *et al.* (2023) ‘Holistic monitoring of freshwater and terrestrial vertebrates by camera trapping and environmental DNA’, *Environmental DNA*, 5(6), 1608–1622. https://doi.org/10.1002/edn3.481.

Høye, T.T. *et al.* (2021) ‘Deep learning and computer vision will transform entomology’, *Proceedings of the National Academy of Sciences of the United States of America*, 118(2). https://doi.org/10.1073/PNAS.2002545117.

Kaplan, M.B. *et al.* (2015) ‘Coral reef species assemblages are associated with ambient soundscapes’, *Marine Ecology Progress Series*, 533, 93–107. https://doi.org/10.3354/meps11382.

Kaspari, M. *et al.* (2022) ‘Activity density at a continental scale: What drives invertebrate biomass moving across the soil surface?’, *Ecology*, 103(1), p. e03542. https://doi.org/10.1002/ecy.3542.

Lamb, P.D. *et al.* (2019) ‘How quantitative is metabarcoding: A meta-analytical approach’, *Molecular Ecology*, 28(2), 420–430. https://doi.org/10.1111/mec.14920.

Leary, P. *et al.* (2023) 'inatVisionAPI'. https://github.com/inaturalist/inatVisionAPI (Accessed: 26 September 2023).

Liu, M. *et al.* (2020) 'A practical guide to DNA metabarcoding for entomological ecologists', *Ecological Entomology*, 45(3), 373–385. https://doi.org/10.1111/een.12831.

Marquina, D. *et al.* (2019) 'Establishing arthropod community composition using metabarcoding: Surprising inconsistencies between soil samples and preservative ethanol and homogenate from Malaise trap catches', *Molecular Ecology Resources*, 19(6), 1516–1530. https://doi.org/10.1111/1755-0998.13071.

Mas-Carrió, E. *et al.* (2022) 'Assessing environmental DNA metabarcoding and camera trap surveys as complementary tools for biomonitoring of remote desert water bodies', *Environmental DNA*, 4(3), 580–595. https://doi.org/10.1002/edn3.274.

Pichler, M. and Hartig, F. (2023) 'Machine learning and deep learning—A review for ecologists', *Methods in Ecology and Evolution*, 14(4), 994–1016. https://doi.org/10.1111/2041-210X.14061.

Ratnasingham, S. and Hebert, P.D.N. (2007) 'BOLD : The Barcode of Life Data System (http://www.barcodinglife.org)', *Molecular Ecology Notes*, 7(3), 355–364. https://doi.org/10.1111/j.1471-8286.2007.01678.x.

Rennstam Rubbmark, O. *et al.* (2018) 'A broadly applicable COI primer pair and an efficient single-tube amplicon library preparation protocol for metabarcoding', *Ecology and Evolution*, 8(24), 12335–12350. https://doi.org/10.1002/ece3.4520.

Sayers, E.W. *et al.* (2024) 'GenBank 2024 Update', *Nucleic Acids Research*, 52(D1), D134–D137. https://doi.org/10.1093/nar/gkad903.

Schneider, S. *et al.* (2022) 'Bulk arthropod abundance, biomass and diversity estimation using deep learning for computer vision', *Methods in Ecology and Evolution*, 13(2), 346–357. https://doi.org/10.1111/2041-210X.13769.

Shea, M.M. *et al.* (2023) 'Systematic review of marine environmental DNA metabarcoding studies: toward best practices for data usability and accessibility', *PeerJ*, 11, p. e14993. https://doi.org/10.7717/peerj.14993.

Stewart, K.A. and Taylor, S.A. (2020) 'Leveraging eDNA to expand the study of hybrid zones', *Molecular Ecology*, 29(15), 2768–2776. https://doi.org/10.1111/mec.15514.

Stork, N.E. (2018) 'How Many Species of Insects and Other Terrestrial Arthropods Are There on Earth?', *Annual Review of Entomology*, 63(1), 31–45. https://doi.org/10.1146/annurev-ento-020117-043348.

Sys, S. *et al.* (2022) 'COLLEMBOLAI , a macrophotography and computer vision workflow to digitize and characterize samples of soil invertebrate communities preserved in fluid', *Methods in Ecology and Evolution*, 13(12), 2729–2742. https://doi.org/10.1111/2041-210X.14001.

Taberlet, P. *et al.* (2012) ‘Towards next-generation biodiversity assessment using DNA metabarcoding’, *Molecular Ecology*, 21(8), 2045–2050. https://doi.org/10.1111/j.1365-294X.2012.05470.x.

Taberlet, P. *et al.* (2018) *Environmental DNA: for biodiversity research and monitoring*. First edition. Oxford, United Kingdom: Oxford University Press.

Takeuchi, Y. *et al.* (2021) ‘The Asia-Pacific Biodiversity Observation Network: 10-year achievements and new strategies to 2030’, *Ecological Research*, 36(2), 232–257. https://doi.org/10.1111/1440-1703.12212.

Terry, J.C.D., Roy, H.E. and August, T.A. (2020) ‘Thinking like a naturalist: Enhancing computer vision of citizen science images by harnessing contextual data’, *Methods in Ecology and Evolution*, 11(2), 303–315. https://doi.org/10.1111/2041-210X.13335.

U.S. Geological Survey (2013) ‘Integrated Taxonomic Information System (ITIS)’. https://doi.org/10.5066/F7KH0KBK.

Wedding, L.M. *et al.* (2019) ‘Remote sensing of three-dimensional coral reef structure enhances predictive modeling of fish assemblages’, *Remote Sensing in Ecology and Conservation*, 5(2), 150–159. https://doi.org/10.1002/rse2.115.

Weiser, M.D. *et al.* (2021) *Batch extraction of morphological and color metrics from invertebrate samples, protocols.io*. https://doi.org/dx.doi.org/10.17504/protocols.io.byt4pwqw.

Weiser, M.D. *et al.* (2022) ‘Robust metagenomic evidence that local assemblage richness increases with latitude in ground-active invertebrates of North America’, *Oikos*, 2022(8), p. e08791. https://doi.org/10.1111/oik.08791.

Wilcox, T.M. *et al.* (2015) ‘The Dual Challenges of Generality and Specificity When Developing Environmental DNA Markers for Species and Subspecies of Oncorhynchus’, *PLOS ONE*. Edited by A.R. Mahon, 10(11), p. e0142008. https://doi.org/10.1371/journal.pone.0142008.

Wood, J.R. *et al.* (2017) ‘No single driver of biodiversity: divergent responses of multiple taxa across land use types’, *Ecosphere*, 8(11), p. e01997. https://doi.org/10.1002/ecs2.1997.